Predominant transport paths of Saharan dust over the Mediterranean Sea to Europe

P. Israelevich,[1] E. Ganor,[1] P. Alpert,[1] P. Kishcha,[1] and A. Stupp[1]

Received 28 June 2011; revised 17 November 2011; accepted 19 November 2011; published 27 January 2012.

[1] We use monthly data of aerosol optical thickness (AOT) from the Moderate Resolution Imaging Spectroradiometer on board the seven NASA Terra and Aqua satellites for a 10 year period (2001–2010) in order to determine seasonal variations of Saharan dust transport over the Mediterranean toward Europe. The maxima of AOT are used to visualize the transport paths. Saharan dust reaches Europe over the Mediterranean and also by looping back over the Atlantic. In spring, aerosols are observed within a wide range of longitudes in Europe, with the highest AOT over western Europe. This may be partially explained by dust transport to western Europe via the Atlantic route, while to central and eastern Europe, dust is transported over the Mediterranean. During all seasons, dust is transported over the Mediterranean to Europe. In the summer months, aerosols are observed predominantly in central Europe. In autumn, aerosol activity is strongest in eastern Europe. We show that there are local AOT maxima over north Italy, in the Alps, in Spain, southeast of the Pyrenees and Sierra Nevada, and in the Rila Mountains in Bulgaria. We suggest that these maxima of aerosol concentration appear as the dust-carrying airflow reaches the mountains and slows.

Citation: Israelevich, P., E. Ganor, P. Alpert, P. Kishcha, and A. Stupp (2012), Predominant transport paths of Saharan dust over the Mediterranean Sea to Europe, *J. Geophys. Res.*, *117*, D02205, doi:10.1029/2011JD016482.

1. Introduction

[2] The Sahara desert is one of the major producing regions of dust particles affecting the radiative budget in the Earth's atmosphere. Most of the Saharan dust is transported over the Atlantic Ocean toward the Americas by trade winds [*Prospero*, 1999]. However, a significant fraction of the dust load from African sources participates in atmospheric circulation above the Mediterranean Sea and Europe [*Engelstaedter et al.*, 2006; *Engelstaedter and Washington*, 2007; *Ganor et al.*, 2000; *Goudie and Middleton*, 2001; *Barkan et al.*, 2004b, 2005]. Desert dust aerosol may impact regional climate, the biogeochemical cycle, and human environments (even mortality rate [e.g., *Sajani et al.*, 2010; *Perez et al.*, 2008]). The aerosol affects the atmosphere both directly by changing reflection and absorption of the solar radiation and indirectly by influencing cloud albedo, precipitation development and cloud lifetime [*Levin et al.*, 1996; *Wurzler et al.*, 2000; *Rosenfeld et al.*, 2001; *Yin et al.*, 2002].

[3] There are no desert dust sources in Europe, nevertheless, the desert dust was observed, at least occasionally, in different regions of Europe [e.g., *Littmann and Steinrucke*, 1989; *Barnaba and Gobbi*, 2004; *Koltay et al.*, 2006; *Perez et al.*, 2008; *Pieri et al.*, 2010; *Sajani et al.*, 2010; *Gerasopoulos et al.*, 2011]. The events with high aerosol optical thickness (AOT) in this region are associated with biomass burning (not only in Europe, smoke from North America may also reach the continent), anthropogenic pollution, soil erosion, transported dust from Sahara sources and volcanic ash. Except the latter, all of them are expected to reveal seasonal variations [*Escudero et al.*, 2005; *Querol et al.*, 2009; *Papayannis et al.*, 2008].

[4] Desert dust transport in the Mediterranean region exhibits distinct long-term climate-controlled [*Jilbert et al.*, 2010] and annual variability [*Moulin et al.*, 1997, 1998; *Barkan et al.*, 2004b; *Barnaba and Gobbi*, 2004; *Engelstaedter and Washington*, 2007]. Annual changes are primarily determined by two independent factors: (1) seasonal dependence of dust sources strength in Africa [*Barkan and Alpert*, 2008] and (2) seasonal changes in the atmospheric circulation [*Israelevich et al.*, 2002; *Barkan et al.*, 2004a]. Comprehensive statistical study of dust episodes [*Ganor et al.*, 2010; *Gkikas et al.*, 2009] reveals a clear difference between eastern and western Mediterranean in aerosol activity and its seasonal dependence. The dynamics of individual aerosol events can be followed using satellite observations (Total Ozone Mapping Spectrometer, TOMS, and Moderate Resolution Imaging Spectroradiometer, MODIS) or model simulations (e.g., DREAM) thus revealing aerosol trajectories for the 55 specific cases [*Kishcha et al.*, 2008]. In spring and summer the air over North Africa is almost permanently loaded with significant amounts of dust. This dust is mobilized and transported northward and eastward along the Mediterranean coast [*Ganor et al.*, 2010]. For the eastern Mediterranean the three periods of increased atmospheric dust are in spring (March–May), in summer (July–August) and in autumn (September–November) [*Israelevich et al.*, 2003]. Aerosol

[1]Department of Geophysics and Planetary Sciences, Tel Aviv University, Tel Aviv, Israel.

0148-0227/12/2011JD016482

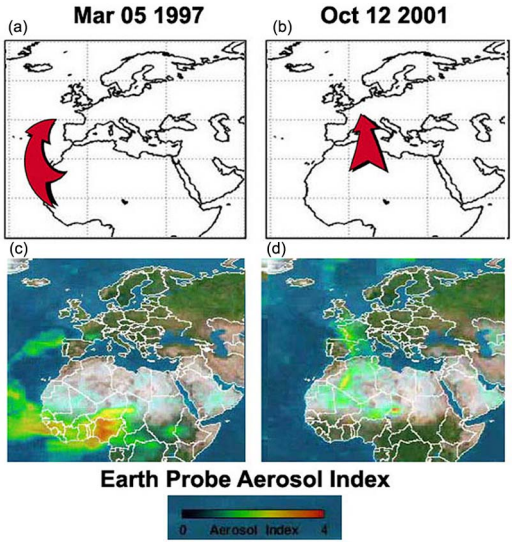

Figure 1. (a, b) Transport paths for desert dust from North Africa to western Europe for Atlantic path and Mediterranean path, respectively. (c, d) Distribution of Total Ozone Mapping Spectrometer (TOMS) aerosol index corresponding to Atlantic path (5 March 1997) and Mediterranean path (12 October 2001), respectively.

vertical distribution exhibits different behavior during these periods [*Kalivitis et al.*, 2007]. There is a distinct difference in the particle size distributions and the real and imaginary parts of the refractive indices for these periods indicating that different dust sources play major role during different seasons [*Israelevich et al.*, 2003].

[5] Each case of desert dust presence in Europe is associated with a certain trajectory of dust-loaded air mass. These individual trajectories differ significantly from event to event. The primary goal of this study is to determine (1) whether there are predominant transport paths by which the dust from North Africa reaches Europe, and (2) if so, do these paths exhibit seasonal variations. The transport paths or routes considered in this study are not trajectories, but rather regions where the trajectories occur with highest probability. AOT maxima are used to visualize the aerosol transport route. In accordance with the continuity equation, local maxima of averaged over long time period AOT appear either above the aerosol source or in the region where the divergence of horizontal aerosol containing flow has minimum [*Israelevich et al.*, 2002], whereas the band of increased average AOT visualizes the typical aerosol transport route during the period of averaging. Obviously, the direction of aerosol propagation is opposite to the AOT gradient, that is, from high to low AOT values. The study is carried out by analyzing 10 year mean distributions of MODIS AOT over the Mediterranean and Europe in different seasons.

2. Data

[6] The idea to use satellite aerosol data in order to investigate major routes of Saharan dust transport toward Europe is illustrated in Figure 1. There are two ways for dust from Africa to reach western Europe. A dust plume intruding into the Atlantic Ocean may turn to the North and then be swept eastward toward Europe as shown in Figure 1a. Desert aerosol may also move directly into Europe over the Mediterranean (Figure 1b). Both transport possibilities occur. Figures 1c and 1d show the distributions of TOMS aerosol index on 5 March 1997 (Atlantic path) and on 12 October 2001 (Mediterranean path). Systematic statistical studies may help to understand which of the two paths is more common in different seasons.

[7] In order to obtain the aerosol transport paths above the region of interest, we analyze 10 year (2001–2010) average MODIS AOT distributions. We use daily distributions of mean AOT as observed by the Moderate Resolution Imaging Spectroradiometer (MODIS) [*Remer et al.*, 2005] on the Terra and Aqua satellites at $\lambda = 550$ nm from the collection 5 Level-3 (1° gridded) daytime daily data (data sets MOD08 D3 and MYD08 D3) at the data archive at http://ladsweb.nascom.nasa.gov/data/search.html. Daily distributions of OMI UV Aerosol index from the Version-003 of Level-3 Aura/OMI daily global TOMS-Like Total Column Ozone gridded product (OMTO3d) were also used.

[8] The distributions are provided on a geographical grid with a resolution of 1° × 1°. The averaged seasonal distributions were calculated by averaging individual daily distributions for the period 2001–2010 (January 2001 to December 2010 for the Terra satellite, and July 2002 to December 2010 for the Aqua satellite).

[9] It is worth mentioning, that MODIS AOT data are absent for the regions with high albedo, namely for the Sahara desert with its dust sources and for snow covered regions in Europe. Furthermore, MODIS AOT data did not allow us to distinguish between different types of aerosol: desert dust, biomass burning products, anthropogenic industrial pollution, agricultural soil erosion, volcanic ash, sea salt aerosols, etc. Such an ambiguity is, to some extent, intrinsic for any remote measurements of aerosol, and only mineralogical studies allow exact determination of aerosol type. Nevertheless, if the band of enhanced AOT starts from North Africa, it is very probable that it is the path of desert dust transport. Vice versa, the bands starting in Europe are associated with other types of aerosols.

[10] Although the bands of the enhanced averaged AOT visualize major dust transport routes, long-term averaging does not allow us to distinguish individual dust events. Therefore, the attempts to calculate backward trajectories of aerosol motion are superfluous. The same is true for an analysis of meteorological situations. Such an analysis could be helpful for studying some specific dust events. However, it cannot be applied to a dust pattern averaged over a long period of time. In addition, it should be noted that different meteorological situations may result in the same direction of aerosol transport. For example, both a cyclone westward from the dust source and an anticyclone eastward from the source causes northward dust transport. Hence, the long-term average direction of aerosol transport is not necessarily associated with a certain meteorological situation.

3. Strong Dust Events and "Background" Transport

[11] The necessity of this approach, in particular, is based on the fact that strong events provide significant but not the

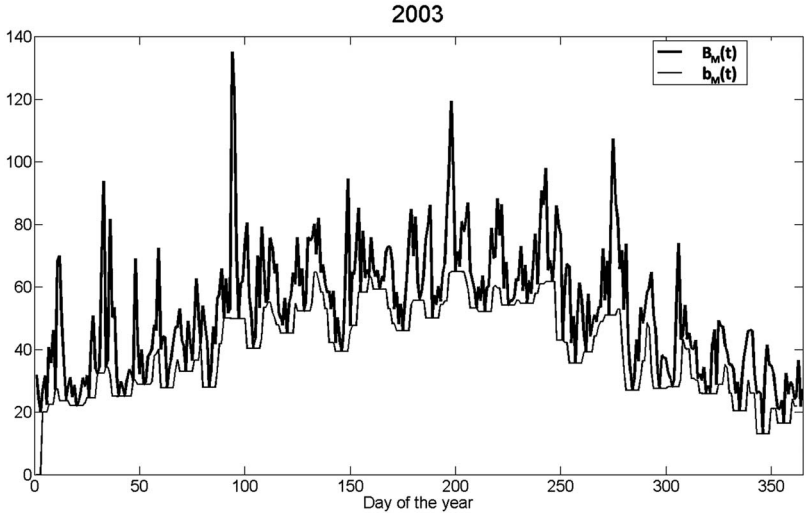

Figure 2. Time dependence of the MODIS AOT integrated over the Mediterranean region, $B_M(t)$, and its lower envelope, $b_M(t)$.

major part of multiyear mean AOD values. According to *Gkikas et al.* [2009], the number of strong events above the Mediterranean with AOT between $\langle AOT \rangle + 2\sigma$ and $\langle AOT \rangle + 4\sigma$ is about seven episodes per year, and there are about three per year extreme events with AOT greater than $\langle AOT \rangle + 4\sigma$. Here $\langle AOT \rangle$ stands for the average AOT and σ stands for the standard deviation. Taking as an estimate σ approximately equal to $\langle AOT \rangle$ and 2 days as the duration of an event [*Ganor*, 1994; *Ganor et al.*, 2010], one estimate that the total aerosol loading during strong aerosol events as follows: $\langle AOT\_STRONG \rangle = (d^*N_s^*AOT_s + d^*N_e^*AOT_e)/365$, where d is the duration of event (estimated as 2 days, N is the number of events per year, indices e and s refer to extremely strong events and strong events, respectively. $N_e = 3$, $N_s = 7$, AOTe is estimated as $5^* \langle AOT \rangle$, AOTs – as $3^* \langle AOT \rangle$. Thus, $\langle AOT\_STRONG \rangle = (2^*3^*7 + 2^*5^*3)/365 = 0.2^* \langle AOT \rangle$; that is, only 20% of total aerosol loading is due to the strong and extremely strong events. Therefore, the major part (80%) of the aerosol loading is produced by smaller events which may even overlap producing almost continuous loading.

[12] In order to determine the relative role of strong dust events in total aerosol transport more accurately, let us consider the daily AOT integrated over the Mediterranean region (0°–40°E, 30°N–40°N):

$$B_M(t_i) = \int_{30}^{40}\int_{0}^{40} AOT(t_i, \varphi, \lambda) d\varphi d\lambda. \quad (1)$$

The time dependence of this measure of the aerosol amount in the atmosphere for 2003 is shown in Figure 2 (thick line). The thin line in Figure 2 shows the lower envelope $b_M(t)$ of the curve $B_M(t)$. Whereas the integral of $B_M(t)$) over the time gives the total amount of aerosol in the atmosphere during the period, the integral of $b_M(t)$ estimates the amount in absence of dust events. The ratio $\int_{year} b_M(t)dt / \int_{year} B_M(t)dt$ is shown in Figure 3 (solid line). The amount of the aerosol in the atmosphere during strong dust events appeared to be 25–30%, which is in good agreement with the crude estimate made in section 1. The same calculations, but for the region in Europe (15°W–40°E, 48°N–51°N), are presented in Figure 3 by the dashed line. The relative role of days with high AOT is somewhat larger (35–40%) but strong events still cannot be considered as the major part of aerosol loading.

4. Seasonal Patterns of Aerosol Optical Thickness Distribution

4.1. Seasonal Dependence of Aerosol Appearance Probability

[13] First we determine seasons of different dust activity in the Mediterranean. We consider the AOT within the rectangular area between 15°W–40°E, and 30°N–40°N (Figure 4, middle). Monthly averaged aerosol optical thickness is integrated along the meridian for each given longitude λ. In order to diminish the effects of the background (the rectangle includes land areas, and even areas where the data on AOT are absent), the integrated monthly averaged AOT is normalized by its sum during a year:

$$A(t_i, \lambda) = \frac{\int_{30}^{40} AOT(t_i, \varphi, \lambda) d\varphi}{\sum_{i=1}^{12}\int_{30}^{40} AOT(t_i, \varphi, \lambda) d\varphi}, \quad (2)$$

where φ is the latitude and t_i is the month of a year.

[14] The normalized quantity A characterizes the monthly probability of dust loading at the given longitude. The results are shown in Figure 4 (bottom). The horizontal and vertical axes correspond to the longitude and months, respectively. The AOT occurrence A is color coded.

[15] The dust activity region is displaced westward during the period from February till September in compliance with established Mediterranean dust seasonal variations [*Moulin et al.*, 1998; *Israelevich et al.*, 2002]. Vertical lines show approximate boundaries between three regions showing distinctly different AOT seasonal dependence: eastern,

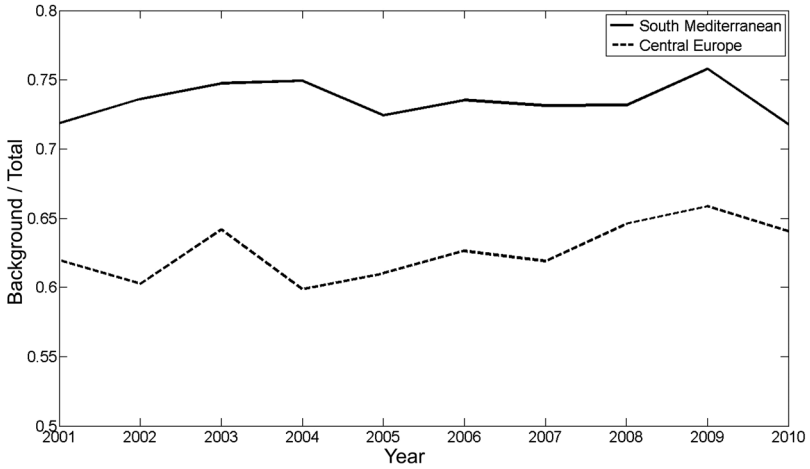

Figure 3. The ratio of background to total aerosol amount for the period 2001–2010. Solid line shows ratio above Mediterranean, and dashed line shows ratio above Europe.

central and western Mediterranean. The same boundaries are shown in Figure 4 (middle). For the whole Mediterranean region, three different seasons (Season I, March–May; Season II, June–July; and Season III, August–September) can be defined. They are emphasized by horizontal lines. In the western sector, there is no clear difference between Seasons II and III, they are rather merged in one season in this region.

[16] A similar analysis is performed for the region in Europe within 15°W–40°E, 48°N–51°N which is also shown in Figure 4 (middle). Noteworthy, the seasons of aerosol activity in this region of Europe are the same as in the Mediterranean, but the geographical distribution of the aerosol episodes is different. First of all, during the Season I, aerosols are observed in Europe in the whole range of longitudes, whereas the dust activity in the western Mediterranean is low. Also, there are two separate maxima of aerosol activity (March and May) in the western part of the selected area (15°W–5°E), especially above the ocean (15°W–5°W). These maxima correspond to the high activity of the Saharan sources in Bodele (∼17°E, 17°N) (March) and El Djouf (∼7°W, 20°N) (May) regions [*Prospero et al.*, 2002; *Israelevich et al.*, 2002; *Koren et al.*, 2006]. If so, the dust in this region is transported over the Atlantic Ocean as shown in Figure 1a. Further eastward transport may also add to the observed AOT in the longitude range 5°E–40°E. However, as it will be shown below, direct dust transport over the Mediterranean to this area is also possible.

[17] During the Season II period, the aerosol activity occurs predominantly in central Europe (5°E–20°E) thus indicating desert aerosol transport over the central Mediterranean. In August–September (Season III), the AOT is highest in the eastern part of Europe (25°E–40°E). These events may be of local origin, but taking into account the fact that during the same period dust activity increases in the eastern Mediterranean the appearance of desert aerosols in eastern Europe cannot be excluded.

4.2. Aerosol Transport Paths

[18] Following *Israelevich et al.* [2002, 2003], the aerosol transport paths above the region of interest are obtained from the following properties of 10 year (2001–2010) average MODIS AOT distributions: positions of local maxima and the bands of the increased AOT. The enhanced AOT bands visualize the dust transport routes. Within the band, direction of propagation is from the region with high AOT to the region with lower AOT. We assume that near the North Africa coast desert dust is the major component of aerosol load [e.g., *Barnaba and Gobbi*, 2004]. We investigate spatial and temporal variations of the 10 year mean AOT above the Mediterranean Sea and Europe, and more specifically over the area extending from 20°N to 70°N and from 30°W to 50°E. We consider the AOT as a measure of amount of aerosol in the air column. Therefore, the AOT integrated over certain area is the measure of the aerosol amount over the region.

[19] Daily AOT distributions are averaged over the three periods denoted in Figure 4. The produced seasonal distributions are given in Figure 5 (left). Arrows in Figure 5 (middle) show the predominant transport of desert aerosol. In the southern Mediterranean, the pattern is similar to that derived from TOMS aerosol index data [*Israelevich et al.*, 2003]. During March–May, dust is transported predominantly eastward. The transport route over the Atlantic Ocean turning eastward to Europe is also visible. In June–July, aerosols from Sahara move northward and westward, whereas dust dynamics in the eastern Mediterranean is determined by "Red Sea sources" on both the African and Arabian coasts of the Red Sea [*Prospero et al.*, 2002; *Israelevich et al.*, 2003]. General features remain the same in August–September with further displacement of activity westward.

[20] In the central Mediterranean, aerosol transport is predominantly northward during all three periods. In this region, dust transport to Europe is less significant in March–May, being the strongest during the June–July period. The predominant direction of dust transport is northwest-westward.

[21] In Seasons II and III, AOT average distributions over central Europe are similar. In August–October, a significant amount of aerosols is observed over eastern Europe (55°N, 25°E–30°E) (Figure 5, bottom), whereas in June–July the average AOT is rather low. In Season III, the region of enhanced aerosol content is connected to dusty regions in

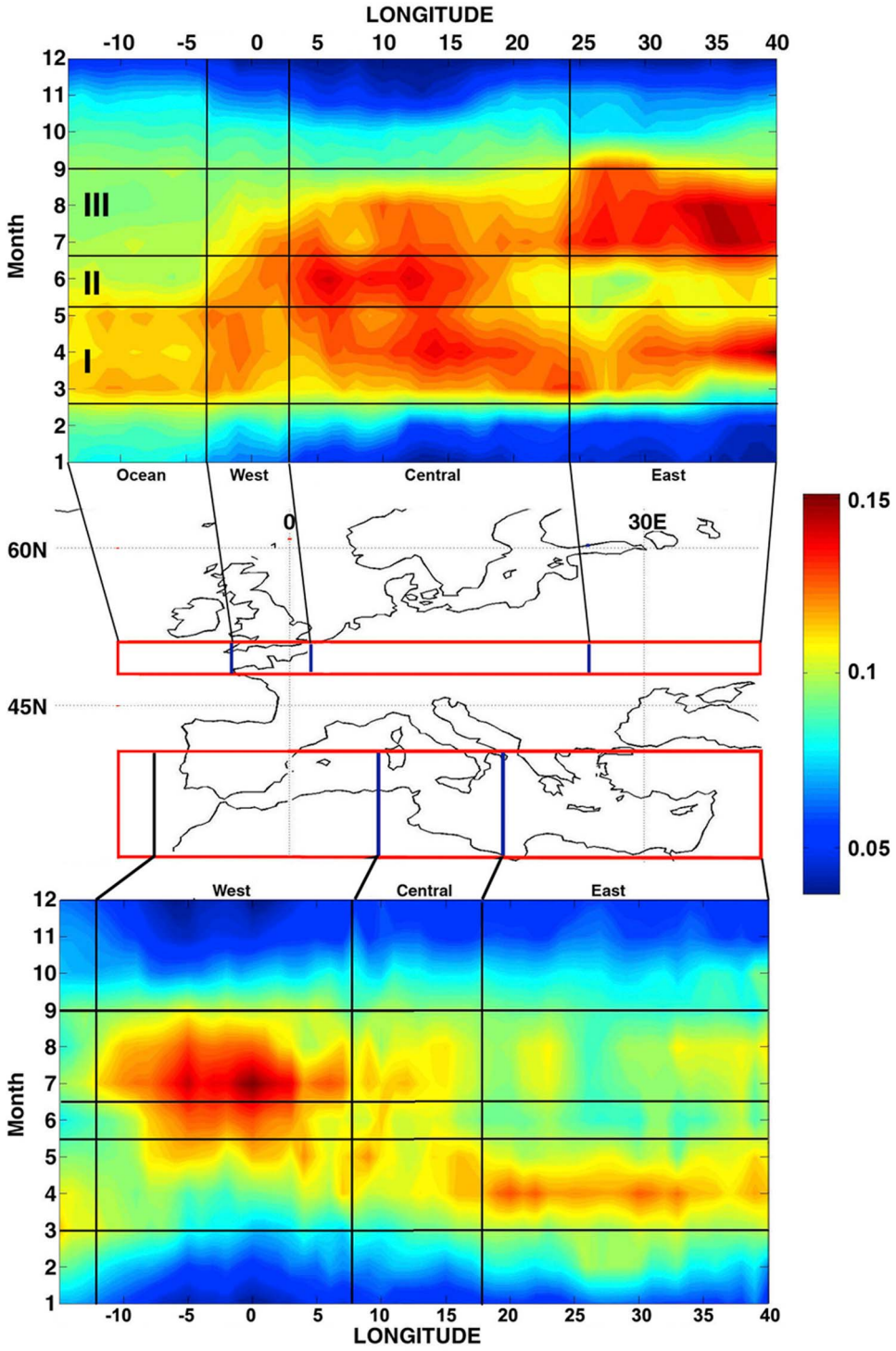

Figure 4. Longitudinal and temporal dependence of the MODIS AOT above two regions: (top) ocean, western Europe, central Europe, and eastern Europe and (bottom) western, central, and eastern Mediterranean. (middle) Maps indicating the two regions (see text for explanation). Vertical lines show approximate boundaries between the regions showing distinctly different AOT seasonal dependence. Three different seasons of aerosol activity are emphasized by horizontal lines in the results for both regions: Season I (spring), Season II (middle summer), and Season III (summer–autumn).

both central Europe and the eastern Mediterranean. Basing only on AOT average distributions, it is impossible to conclude whether aerosols were transported from central Europe, or dust was brought from Middle East sources through the eastern Mediterranean, or both routes were valid for this season.

[22] The local AOT maxima, denoted as A, B, C, and D in Figure 5, are noteworthy. Maximum A is located over north

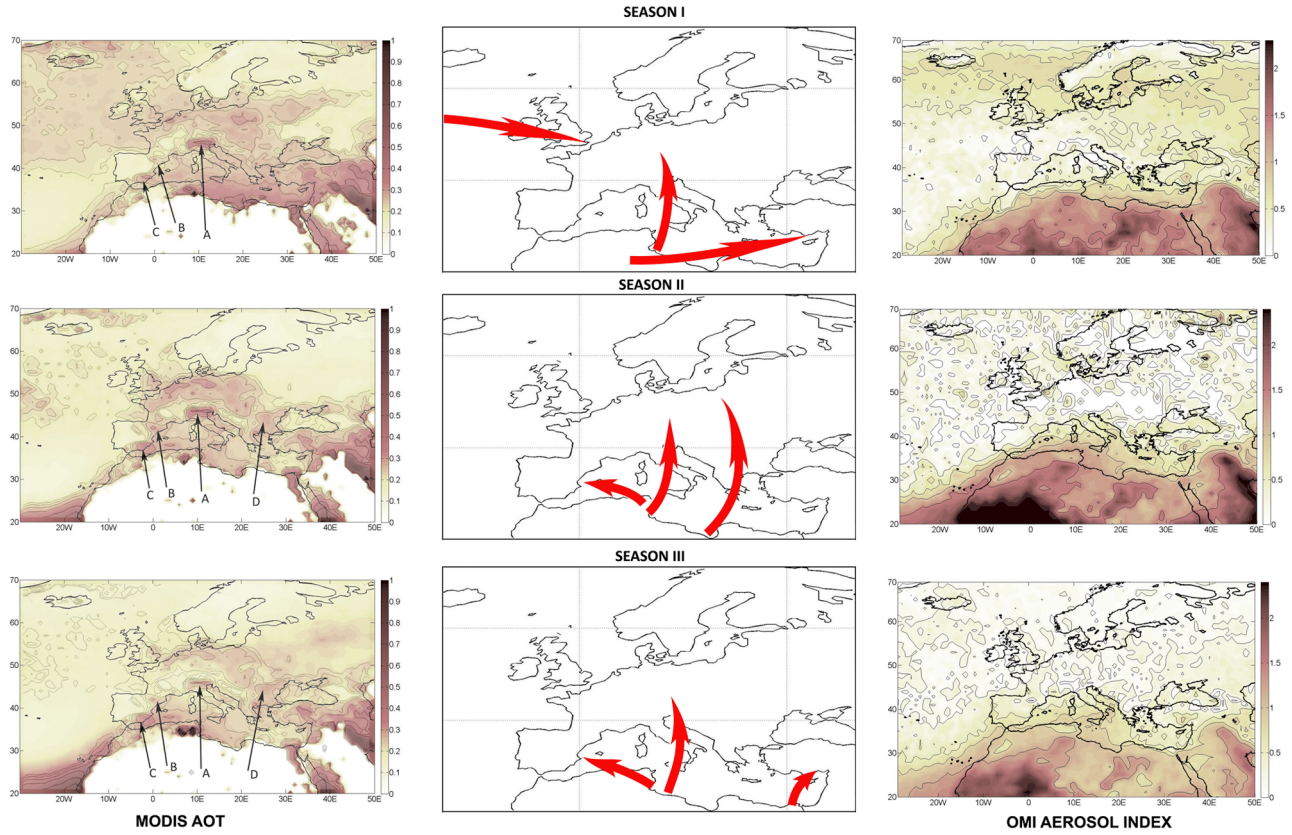

Figure 5. (left) MODIS AOT distributions averaged for Season I (March–May), Season II (June–July), and Season III (August–September). (middle) Cartoons denoting corresponding aerosol transport paths. (right) OMI aerosol index distributions averaged for the same periods.

Italy, south of the Alps, and is observed almost around the whole year, except for January and December. Maximum B is observed southeast of the Pyrenees, C is observed east of Sierra Nevada, and D is observed south of the Rila Mountains. The existence of these maxima might be a manifestation of desert dust transport over the Mediterranean to Europe. Indeed, if the dust-carrying flow decelerates as it approaches the mountains, the dust concentration and AOT should increase. This can be expected for the Pyrenees (northwest directed dust transport), for Sierra Nevada (westward transport), for the Rila (northward transport), and for the Alps (also northward transport). This effect will be discussed in section 5.

[23] Aerosol index (AI) [*Torres et al.*, 1998, 2007] can be considered as another measure of the aerosol amount in the air column. It is not as sensitive to surface albedo as MODIS AOT and is obtained (contrary to MODIS AOT) for the regions with high reflectance in Sahara desert. By definition, positive values of AI correspond to absorbing aerosols. As compared to MODIS AOT, aerosol index is relatively more sensitive to coarse mode particles and, because of Rayleigh scattering to high-altitude aerosol layers. Therefore, is interesting to compare the pattern of transport paths derived from MODIS AOT (Figure 5) with AI data. We apply the same procedure to OMI AI for the years (2004–2010) and consider the bands of enhanced average OMI AI as transport path. The results are shown in Figure 5 (right). Along the transport paths, the AI decreases faster than MODIS AOT. In general, it is explained by the change of particle size distribution: over Europe the ratio of coarse mode to fine mode drops as the relative role of anthropogenic aerosols becomes more significant. Above the Mediterranean, where OMI is high enough, the general pattern remains the same as that in Figure 5 (left) (MODIS AOT distributions), with the same seasonal trend. However, the total absence of maxima in front of the mountains assumes that the aerosol layers producing these maxima are too low in order the presence can be revealed in UV.

[24] Since the amount of aerosol transported during the dusty days is comparable with the background transport during relatively quiet periods, it is instructive to compare "events" and "background" transport paths.

[25] All daily AOT data are separated in two groups. We define as a "dusty event" the day when daily AOT, integrated over the Mediterranean region (0°–40°E, 30°N–40°N), was at least 20% larger than its 30 day average level. The first group includes all dusty days plus 2 days immediately following the dusty one. The latter is done in order not to miss the days when the aerosol cloud leaves the region of integration but still may exist. The rest of the days are included in the second group of nondusty days.

[26] Figure 6 shows the AOT distributions averaged over dusty (Figure 6, middle) and nondusty (Figure 6, right) days, along with the distributions averaged over the whole seasons (Figure 6, left). Top maps correspond to the Season I, middle

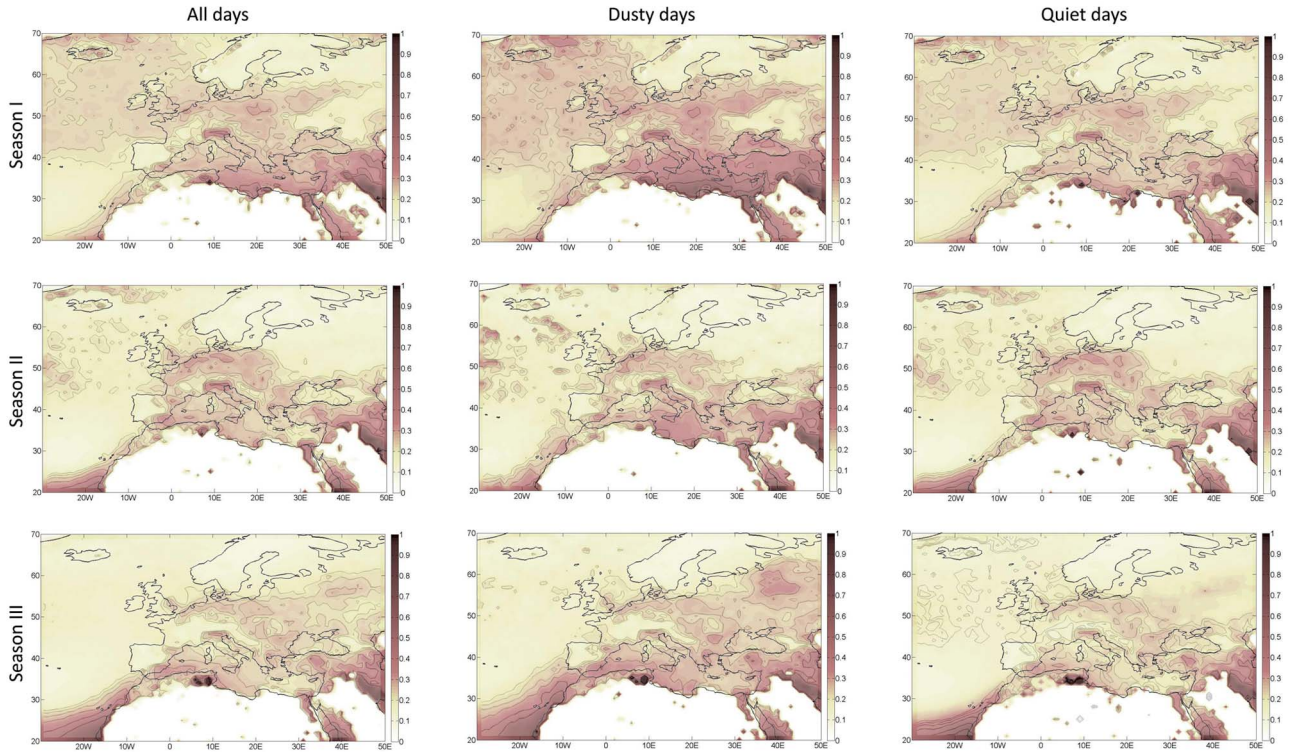

Figure 6. (left) MODIS AOT distributions averaged over the whole season. (middle) MODIS AOT distributions averaged over dusty days. (right) MODIS AOT distributions averaged over nondusty days. Results are shown for Season I, Season II, and Season III.

maps correspond to the Season II, and bottom maps correspond to Season III.

[27] Analysis of Figure 6 reveals that the transport routes for "dusty" and "nondusty" days are similar with two exceptions. First, the transport in eastern Mediterranean is different on dusty days and on nondusty days in Season I. Strong dust events propagate along the African coast eastward, whereas this transport path disappears on the days low dust activity. The high dust loading is a consequence of the Sharav cyclone and the eastward dust path visualizes the motion of the cyclone [*Alpert and Ziv*, 1989; *Israelevich et al.*, 2002]. Therefore, selecting days with high dust loading, we, in fact, select days with the Sharav cyclone and dust transport to eastern Mediterranean. On nondusty days (the second group), the Sharav cyclone is absent and there is no eastward transport.

[28] Second, in Season III, Mediterranean dust events, that is, the increased AOT over the Mediterranean (0°–40°E, 30°N–40°N), are accompanied by increased AOT in eastern Europe (35°–45°E, 52°N−58°N). On nondusty days (the second group), aerosol activity in eastern Europe also remains low. This is an argument in favor of possibility of Mediterranean dust transport to eastern Europe.

5. Aerosol Transport and Mountains

[29] The local AOT should increase if the horizontal flow carrying aerosols is decelerated in front of mountains. As it was mentioned at the end of section 3, this mechanism might be responsible for local maxima of AOT near the Alps, Pyrenees, Sierra Nevada and Rila shown in Figure 5. On the other hand, these maxima may be produced by local aerosol sources like industrial pollution, soil erosion etc. Let us consider the enhancement of AOT in front of the Alps above the Po valley (marked by A in Figure 5). The Season I MODIS AOT distribution fits very well the mountain relief of the Alps as it is shown in Figure 7 laying AOT over the satellite image of northern Italy.

[30] Being an industrial region, Po valley is the place of strong anthropogenic industrial pollution [*Barkan et al.*, 2005; *Barnaba and Gobbi*, 2004]. There are also no doubts that significant amounts of desert dust occasionally appear in this region. Dust from Sahara plays the essential role in the neutralization precipitation [*Pieri et al.*, 2010]. Health effects of desert dust presence in Po valley were also observed [*Sajani et al.*, 2010].

[31] Moreover, deceleration of the northward dust-carrying flow from the central Mediterranean near the Alps may also create a kind of "trap" resulting in an increase of dust 244 concentration and AOT maximum in this region, as observed by MODIS instrument (Figure 5). For example, aerosol was trapped in the Po valley on 13 October 2001, and the results of aerosol mask application to the region above the Adriatic Sea adjacent to Po valley show that the aerosol in the "trap" is mainly desert dust [see *Barnaba and Gobbi*, 2004, Figure 5].

[32] Figure 8 shows monthly averaged AOT integrated over the region 44°–46°N, 7°–14°E (north Italy). The largest values are observed in the April–June period, which is typical for the central Mediterranean as it can be expected for desert dust transport through the Mediterranean to Europe.

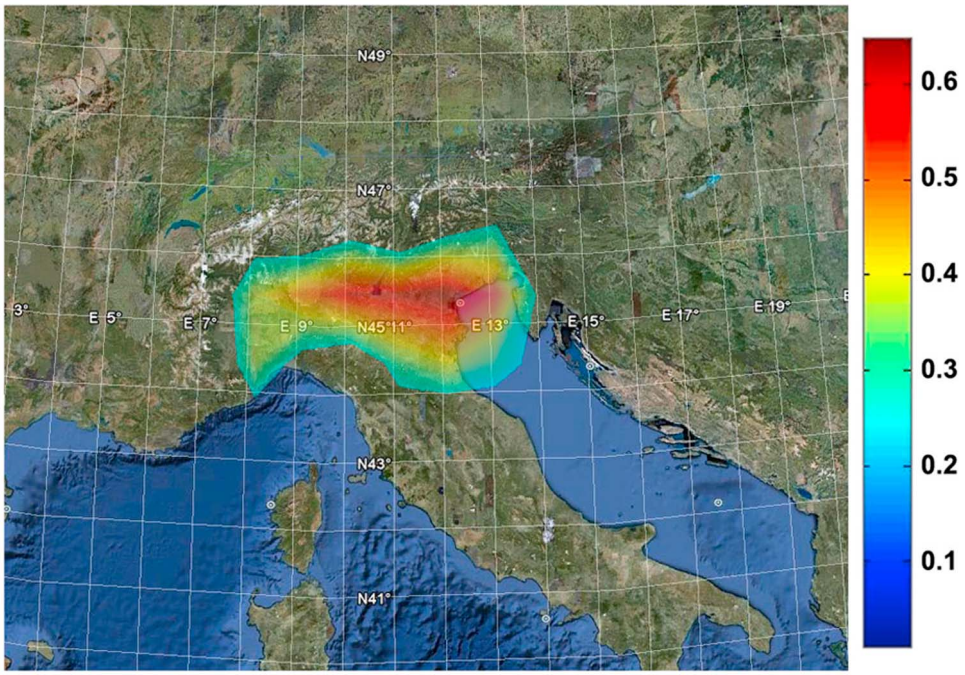

Figure 7. Spring MODIS AOT distribution superimposed on the satellite image of southern Europe. Only regions with AOT larger than 0.25 are shown.

[33] In order to verify this assumption, we consider in the region 7°E–15°E, 30°N–55°N (Figure 9, top) the daily AOT integrated over the longitude:

$$C(t_i, \varphi) = \int_7^{15} AOT(t_i, \varphi, \lambda) d\lambda. \quad (3)$$

The results of $C(t, \varphi)$ calculations for the year 2008 are presented in Figure 9 (middle). Figure 9 (bottom) shows a part of Figure 9 (middle) in increased scale.

[34] Being rather short (~2 days), dust events are distributed continuously along wide range of latitudes. A clear increase of AOT can be seen near the latitude of the Southern Alps denoted by the arrow, as it should be for the decelerated northward flow. Also, there are no enhancements of AOT above the Po valley which are not extended southward. Sources of industrial pollution operate rather continuously. Therefore, if the AOT maxima are produced by pollution, one can expect that they should be prominent, when the aerosol transport with air masses is weak or absent, and they should decrease in cases, when the aerosol is

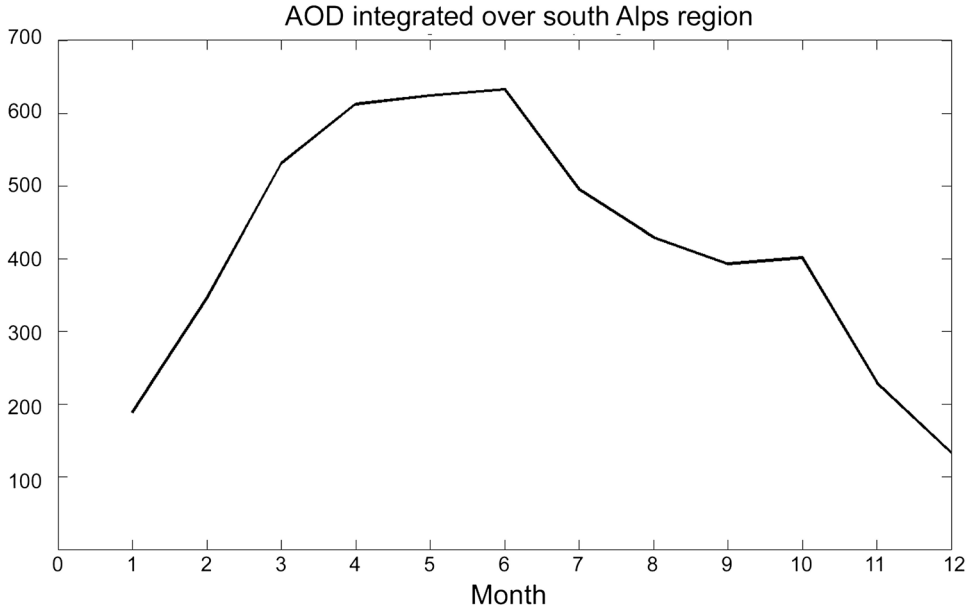

Figure 8. The average seasonal variation of MODIS AOT in north Italy.

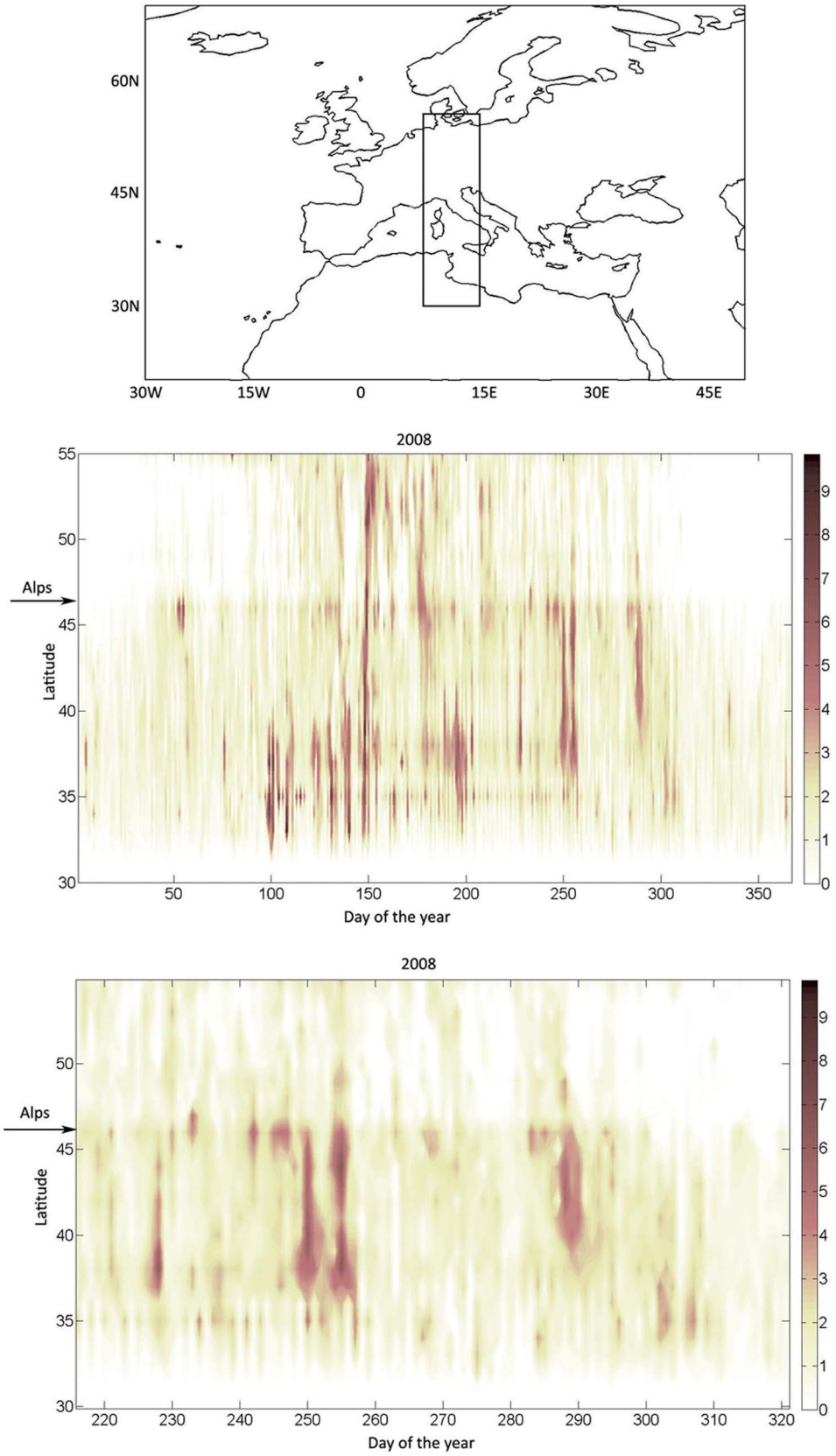

Figure 9. Dependence on time and latitude of daily MODIS AOT integrated over longitude (top) inside the region 7°E–15°E, 30°N–55°N, (middle) for the year 2008, and (bottom) for an the period 1 August to 15 November 2008. Arrows denote the latitude of Southern Alps' spurs.

distributed over larger areas owing to the transport motion. Figure 9 demonstrates quite opposite behavior. The aerosol amount above the Po valley usually increases for the events with latitude spread. Thus, we conclude that the effect of flow deceleration by mountain relief, causing AOT increase, indeed takes place.

6. Conclusion

[35] Our analysis of monthly averaged AOT distributions over Europe for the period 2001–2010 revealed three seasons of aerosol activity above the continent. They coincide with three distinct seasons of desert dust activity in the Mediterranean region, namely, March–May, June–July and August–September. Over western Europe (15°W–5°E), AOT is the highest in spring, contrary to the western Mediterranean where the highest AOT is observed in autumn. In spring, the predominant dust transport route from Saharan sources to western Europe is a westward motion of dust plumes by trade winds, with subsequent turn northward and then back to the East. Over central Europe (5°E–25°E) the aerosol activity has two maxima, in the spring and summer seasons, whereas over eastern Europe (25°–40°E) AOT is highest in spring and autumn. The dust is brought to these sectors from the eastern Mediterranean by air masses moving northward.

[36] The existence of aerosol transport routes toward Europe is manifested by the appearance of localized regions of increased average AOT on the Mediterranean side of mountain ranges (the Alps, Rila, Pyrenees, Sierra Nevada). In those regions, AOT increases owing to deceleration of the horizontal flow carrying aerosols in front of the mountains.

[37] **Acknowledgments.** MODIS-Terra and MODIS-Aqua daily data of aerosol optical thickness data at 550 nm were obtained from NASA's MODIS Data Processing System (MODAPS) Web site (http://ladsweb.nascom.nasa.gov/data/search.html). Daily data of OMI Aerosol Index were obtained from Giovanni online data system, developed and maintained by the NASA GES DISC. We acknowledge the mission scientists and Principal Investigators who provided the data used in this research effort.

References

Alpert, P., and B. Ziv (1989), The Sharav Cyclone: Observation and some theoretical considerations, *J. Geophys. Res.*, *94*, 18,495–18,514, doi:10.1029/JD094iD15p18495.

Barkan, J., and P. Alpert (2008), Synoptic patterns associated with dusty and non-dusty seasons in the Sahara, *Theor. Appl. Climatol.*, *94*, 153–162, doi:10.1007/s00704-007-0354-9.

Barkan, J., H. Kutiel, P. Alpert, and P. Kishcha (2004a), Synoptics of dust intrusion days from the African continent into the Atlantic Ocean, *J. Geophys. Res.*, *109*, D08201, doi:10.1029/2003JD004416.

Barkan, J., H. Kutiel, and P. Alpert (2004b), Climatology of dust sources in North Africa and the Arabian Peninsula based on TOMS data, *Indoor Built Environ.*, *13*, 407–419, doi:10.1177/1420326X04046935.

Barkan, J., P. Alpert, H. Kutiel, and P. Kishcha (2005), Synoptics of dust transportation days from Africa toward Italy and central Europe, *J. Geophys. Res.*, *110*, D07208, doi:10.1029/2004JD005222.

Barnaba, F., and G. P. Gobbi (2004), Aerosol seasonal variability over the Mediterranean region and relative impact of maritime, continental and Saharan dust particles over the basin from MODIS data in the year 2001, *Atmos. Chem. Phys.*, *4*, 2367–2391, doi:10.5194/acp-4-2367-2004.

Engelstaedter, S., and R. Washington (2007), Atmospheric controls on the annual cycle of North African dust, *J. Geophys. Res.*, *112*, D03103, doi:10.1029/2006JD007195.

Engelstaedter, S., I. Tegen, and R. Washington (2006), North African dust emissions and transport, *Earth Sci. Rev.*, *79*, 73–100, doi:10.1016/j.earscirev.2006.06.004.

Escudero, M., S. Castillo, X. Querol, A. Avila, M. Alarcon, M. M. Viana, A. Alastuey, E. Cuevas, and S. Rodriguez (2005), Wet and dry African dust episodes over eastern Spain, *J. Geophys. Res.*, *110*, D18S08, doi:10.1029/2004JD004731.

Ganor, E. (1994), The frequency of Saharan dust episodes over Tel Aviv, Israel, *Atmos. Environ.*, *28*, 2867–2871, doi:10.1016/1352-2310(94)90087-6.

Ganor, E., Y. Deutsch, and H. A. Foner (2000), Mineralogical composition and sources of airborne settling particles on Lake Kinneret (the sea of Galilee) in Israel, *Water Air Soil Pollut.*, *118*, 245–262, doi:10.1023/A:1005167230795.

Ganor, E., I. Osetinsky, A. Stupp, and P. Alpert (2010), Increasing trend of African 315 dust, over 49 years, in the eastern Mediterranean, *J. Geophys. Res.*, *115*, D07201, doi:10.1029/2009JD012500.

Gerasopoulos, E., V. Amiridis, S. Kazadzis, P. Kokkalis, K. Eleftheratos, M. O. Andreae, T. W. Andreae, H. El-Askary, and C. S. Zerefos (2011), Three-year ground based measurements of aerosol optical depth over the Eastern Mediterranean: The urban environment of Athens, *Atmos. Chem. Phys.*, *11*, 2145–2159, doi:10.5194/acp-11-2145-2011.

Gkikas, A., N. Hatzianastassiou, and N. Mihalopoulos (2009), Aerosol events in the broader Mediterranean basin based on 7-year (2000–2007) MODIS C005 data, *Ann. Geophys.*, *27*, 3509–3522, doi:10.5194/angeo-27-3509-2009.

Goudie, A. S., and N. J. Middleton (2001), Saharan dust storms: Nature and consequences, *Earth Sci. Rev.*, *56*, 179–204, doi:10.1016/S0012-8252(01)00067-8.

Israelevich, P. L., Z. Levin, J. H. Joseph, and E. Ganor (2002), Desert aerosol transport in the Mediterranean region as inferred from the TOMS aerosol index, *J. Geophys. Res.*, *107*(D21), 4572, doi:10.1029/2001JD002011.

Israelevich, P. L., E. Ganor, Z. Levin, and J. H. Joseph (2003), Annual variations of physical properties of desert dust over Israel, *J. Geophys. Res.*, *108*(D13), 4381, doi:10.1029/2002JD003163.

Jilbert, T., G.-J. Reichart, B. Aeschlimann, D. Günther, W. Boer, and G. de Lange (2010), Climate-controlled multidecadal variability in North African dust transport to the Mediterranean, *Geology*, *38*, 19–22, doi:10.1130/G25287.1.

Kalivitis, N., E. Gerasopoulos, M. Vrekoussis, G. Kouvarakis, N. Kubilay, N. Hatzianastassiou, I. Vardavas, and N. Mihalopoulos (2007), Dust transport over the eastern Mediterranean derived from Total Ozone Mapping Spectrometer, Aerosol Robotic Network, and surface measurements, *J. Geophys. Res.*, *112*, D03202, doi:10.1029/2006JD007510.

Kishcha, P., S. Nickovic, E. Ganor, L. Kordova, and A. Alpert (2008), Saharan dust over the Eastern Mediterranean: Model sensitivity, in *Air Pollution Modeling and Its Applications*, vol. 19, chap. 4.2, pp. 358–366, Springer, New York, doi:10.1007/978-1-4020-8453-9_39.

Koltay, E., I. Borbély-Kiss, Z. Kertész, A. Z. Kiss, and G. Szabó (2006), Assignment of Saharan dust sources to episodes in Hungarian atmosphere by PIXE and TOMS observations, *J. Radioanal. Nucl. Chem.*, *267*, 449–459, doi:10.1007/s10967-006-0073-1.

Koren, I., Y. J. Kaufman, R. Washington, M. C. Todd, Y. Rudich, J. Vanderlei Martins, and D. Rosenfeld (2006), The Bodélé depression: A single spot in the Sahara that provides most of the mineral dust to the Amazon forest, *Environ. Res. Lett.*, *1*, 014005, doi:10.1088/1748-9326/1/1/014005.

Levin, Z., E. Ganor, and V. Gladstein (1996), The effects of desert particles coated with sulfate on rain formation in the eastern Mediterranean, *J. Appl. Meteorol.*, *35*, 1511–1523, doi:10.1175/1520-0450(1996)035<1511:TEODPC>2.0.CO;2.

Littmann, T., and J. Steinrucke (1989), Atmospheric boundary conditions of recent Saharan dust influx into Central Europe, *GeoJournal*, *18*, 399–406, doi:10.1007/BF00772694.

Moulin, C., F. Guillard, F. Dulac, and C. E. Lambert (1997), Long-term daily monitoring of Saharan dust load over ocean using Meteosat ISCCP-B2 data: 1. Methodology and preliminary results for 1983–1994 in the Mediterranean, *J. Geophys. Res.*, *102*, 16,947–16,958, doi:10.1029/96JD02620.

Moulin, C., et al. (1998), Satellite climatology of African dust transport in the Mediterranean atmosphere, *J. Geophys. Res.*, *103*, 13,137–13,144, doi:10.1029/98JD00171.

Papayannis, A., et al. (2008), Systematic lidar observations of Saharan dust over Europe in the frame of EARLINET (2000–2002), *J. Geophys. Res.*, *113*, D10204, doi:10.1029/2007JD009028.

Perez, L., A. Tobias, X. Querol, N. Künzli, J. Pey, A. Alastuey, M. Viana, N. Valero, M. González-Cabré, and J. Sunyer (2008), Coarse particles from Saharan dust and daily mortality, *Epidemiology*, *19*, 800–807, doi:10.1097/EDE.0b013e31818131cf.

Pieri, L., P. Matzneller, N. Gaspari, I. Marotti, G. Dinelli, and P. Rossi (2010), Bulk atmospheric deposition in the southern Po Valley (northern Italy), *Water Air Soil Pollut.*, *210*, 155–169, doi:10.1007/s11270-009-0238-y.

Prospero, J. M. (1999), Long-term measurements of the transport of African mineral dust to the southeastern United States: Implications for regional air quality, *J. Geophys. Res.*, *104*, 15,917–15,927, doi:10.1029/1999JD900072.

Prospero, J. M., P. Ginoux, O. Torres, S. E. Nicholson, and T. E. Gill (2002), Environmental characterization of global sources of atmospheric soil dust identified with the nimbus 7 total ozone mapping spectrometer (TOMS) absorbing aerosol product, *Rev. Geophys.*, *40*(1), 1002, doi:10.1029/2000RG000095.

Querol, X., et al. (2009), African dust influence on ambient PM levels in South-Western Europe (Spain and Portugal): A quantitative approach to support implementation of Air Quality Directives, *IOP Conf. Ser., Earth Environ. Sci.*, *7*, 012018, doi:10.1088/1755-1307/7/1/012018.

Remer, L. A., et al. (2005), The MODIS aerosol algorithm, products and validation, *J. Atmos. Sci.*, *62*, 947–973, doi:10.1175/JAS3385.1.

Rosenfeld, D., Y. Rudich, and R. Lahav (2001), Desert dust suppressing precipitation: A possible desertification feedback loop, *Proc. Natl. Acad. Sci. U. S. A.*, *98*, 5975–5980, doi:10.1073/pnas.101122798.

Sajani, S. Z., R. Miglio, P. Bonasoni, P. Cristofanelli, A. Marinoni, C. Sartini, C. A. Goldoni, G. De Girolamo, and P. Lauriola (2010), Saharan dust and daily mortality in Emilia-Romagna (Italy), *Occup. Environ. Med.*, *68*, 446–451, doi:10.1136/oem.2010.058156.

Torres, O., P. K. Bhartia, J. R. Herman, Z. Ahmad, and J. Gleason (1998), Derivation of aerosol properties from satellite measurements of backscattered ultraviolet radiation: Theoretical basis, *J. Geophys. Res.*, *103*, 17,099–17,110, doi:10.1029/98JD00900.

Torres, O., A. Tanskanen, B. Veihelmann, C. Ahn, R. Braak, P. K. Bhartia, P. Veefkind, and P. Levelt (2007), Aerosols and surface UV products from Ozone Monitoring Instrument observations: An overview, *J. Geophys. Res.*, *112*, D24S47, doi:10.1029/2007JD008809.

Wurzler, S., T. G. Reisin, and Z. Levin (2000), Modification of mineral dust particles by cloud processing and subsequent effects on drop size distributions, *J. Geophys. Res.*, *105*, 4501–4512, doi:10.1029/1999JD900980.

Yin, Y., S. Wurzler, Z. Levin, and T. Reisin (2002), Interactions of mineral dust particles and clouds: Effects on precipitation and cloud optical properties, *J. Geophys. Res.*, *107*(D23), 4724, doi:10.1029/2001JD001544.

P. Alpert, E. Ganor, P. Israelevich, P. Kishcha, and A. Stupp, Department of Geophysics and Planetary Sciences, Tel Aviv University, Tel Aviv 69978, Israel. (peter@post.tau.ac.il)